NATIONAL ADVISORY COMMITTEE FOR AERONAUTICS

TECHNICAL NOTE 4335

PROCEDURE FOR CALCULATING FLUTTER AT HIGH SUPERSONIC SPEED INCLUDING CAMBER DEFLECTIONS, AND COMPARISON WITH EXPERIMENTAL RESULTS

By Homer G. Morgan, Vera Huckel,
and Harry L. Runyan

Langley Aeronautical Laboratory
Langley Field, Va.

NACA

Washington

September 1958

NATIONAL ADVISORY COMMITTEE FOR AERONAUTICS

TECHNICAL NOTE 4335

PROCEDURE FOR CALCULATING FLUTTER AT HIGH SUPERSONIC SPEED INCLUDING CAMBER DEFLECTIONS, AND COMPARISON WITH EXPERIMENTAL RESULTS

By Homer G. Morgan, Vera Huckel,
and Harry L. Runyan

SUMMARY

A method which may be used at high supersonic Mach numbers is described for calculating the flutter speed of wings having camber in their deflection modes. The normal coupled vibration modes of the wing are used to derive the equations of motion. Chord deflections of the vibration modes are approximated by polynomials. The wing may have a control surface and may carry external stores although no aerodynamic forces on the stores are presented. The aerodynamic forces that are assumed to be acting on the wing are obtained from piston theory and also from a quasi-steady form of a theory for two-dimensional steady flow. Airfoil shape and thickness effects are taken account of in the analysis.

The method is used to calculate the flutter speed of some wings which had been previously tested at Mach numbers of 1.3 to 3.0. Comparison of the calculations and experiment is made for flat-plate 60° and 45° delta wings and also for an untapered 45° sweptback wing.

INTRODUCTION

The requirements for low drag at high speed have led to the use of thin low-aspect-ratio wings. Structural weights must also be minimized to avoid penalizing performance. When such wings are designed primarily for the strength required to carry a given static load, the relative stiffness is considerably reduced, particularly in the resistance to camber deformation. This tendency for wings to deform in camber has introduced a new element in the flutter picture, namely, a need for a method of analysis that can take into account such deformations. Such a procedure should be suitable for programing on digital computing equipment and could be used as a reference calculation for the correlation of data.

In reference 1, several aerodynamic theories were discussed and used in comparative flutter calculations. Piston theory, described in detail in references 2 and 3, was one of the simpler methods discussed. It was shown to give results in agreement with more exact theories when used in two-degree-of-freedom flutter calculations for Mach numbers greater than about 2. It is easily adaptable to the present problem of including camber deformations, because of its inherent simplicity. A quasi-steady aerodynamic method, deduced from second-order steady-flow theory, was also tried for comparison with piston theory. Both of these methods allow the effects of airfoil shape and thickness, which are not treated in the linearized aerodynamic theories, to be included.

In this report a procedure for flutter analysis utilizing the normal (coupled) vibration modes, which include cambering deflections, as the structural input is presented. The first part of the report contains the derivation of the flutter determinant. The second part has the results of several applications to low-aspect-ratio wings and presents a comparison with some experimental results. In order to illustrate the procedure, a sample calculation is given in the appendix.

SYMBOLS

$A_{ij}, B_{ij}, C_{ij}, D_{ij}$ surface integrals of wing properties

a speed of sound, ft/sec

$\left(a_i^{(n)}\right)_p, \left(b_i^{(n)}\right)_q$ coefficients of polynomials approximating mode shape at station n in mode i

b local semichord, ft

F dissipation function (eq. 11)

$f_i(x',y')$ modal function for mode i

$f_i^{(n)}(x)$ polynomial which approximates mode i at station n

$G = \frac{\gamma + 1}{2} M$

$\bar{G} = \frac{(\gamma + 1)M^4 - 4\beta^2}{2\beta^3}$

g	structural damping coefficient
I	number of modes in analysis
I_{α_s}	mass moment of inertia of store in pitch about attachment point, lb-sec^2-ft
K	number of polynomials used to approximate chordwise mass distribution
k	reduced frequency, $b\omega/V$
$k(x',y')$	stiffness influence function, lb/ft/sq ft
l	wing semispan, ft
l_κ	x-coordinate at ends of mass interval
M	Mach number
M_i	generalized mass for mode i
$m(x',y')$	mass per unit area, slugs/sq ft
m_s	mass of store, lb-sec^2/ft
$\left(m^{(n)}\right)_\kappa$	coefficients of polynomials approximating mass distribution at station n in interval κ
n	index indicating spanwise station
N	number of spanwise stations used to approximate wing properties
P,Q	degree of polynomials
p	pressure, lb/sq ft
S_{α_s}	static unbalance of store in pitch about attachment point, lb-sec^2
s_ν,t_ν	thickness terms defined by equation (26)
T	kinetic energy
t	time, sec

U potential energy

V velocity, ft/sec

w downwash velocity, positive measured away from surface, ft/sec

$X = \left(\frac{\omega_1}{\omega}\right)^2 (1 + ig)$

x',y',z' Cartesian coordinates

x,y coordinates along chord, in fraction of local chord, and along span, in fraction of semispan, respectively

x_1 coordinate of flap leading edge, fraction of local chord

$Z(x',y')$ function describing airfoil surface, positive away from mean surface

$Z^{(n)}(x)$ function describing airfoil contour at station n, positive away from airfoil mean line

$z(x',y',t)$ vertical coordinate of deflected wing mean surface, positive up

$\beta = \sqrt{M^2 - 1}$

γ ratio of specific heats

δ_i vertical displacement of deflected wing mean surface at store attachment point in mode i

ϵ_i slope of deflected wing mean surface, relative to undeflected mean surface, in stream direction at store attachment point in mode i

$\mu = \dfrac{\text{Mass of wing}}{\pi\rho \int_0^l b^2 dy'}$

$\xi_i(t)$ generalized coordinate of motion in mode i

$\bar{\xi}_i$ amplitude of generalized coordinate for mode i

ρ	air density, slugs/cu ft
ω	circular frequency, radians/sec
ω_i	ith natural circular frequency

Subscripts:

i,j	indices indicating mode
∞	free stream
p,q,r,s	indices pertaining to terms in polynomials
R	reference
κ	index which denotes the interval along chord over which mass distribution is approximated by a parabola

Superscripts:

1, 2, 3, . . . n	spanwise station

Matrix notation:

$[\ ]$	square
$\begin{bmatrix} \searrow \end{bmatrix}$	diagonal

A dot over a symbol indicates differentiation with respect to time.

ANALYSIS

In order to develop the procedure, certain classical methods of flutter analysis are to be applied. Consider a wing of arbitrary plan form whose mass, stiffness, and geometric properties are known. A right-hand coordinate system x',y',z', as shown in figure 1, with the origin at the leading edge of the wing root is used to describe these properties. The wing has a flap which is hinged about its own leading edge. The airfoil shape is described by a surface $Z(x',y')$ which is measured from the mean surface of the wing and is taken as positive away from the mean surface. The mass distribution is $m(x',y')$, the mass per unit area at any point on the wing. The stiffness influence function is $k(x',y')$, an equivalent spring constant at any point on the surface.

Derivation of Equations of Motion

Assume that the deflections can be described by superposing the first I vibration modes of the wing. It is assumed for convenience that these modes are normal modes. Then, if $f_i(x',y')$ is the model function describing the deflected position of the mean surface in the ith mode and $\xi_i(t)$ is the corresponding time-dependent generalized coordinate, the complete description of the position of the wing is

$$z(x',y',t) = \sum_{i=1}^{I} f_i(x',y')\xi_i(t) \tag{1}$$

With the position of each point so described, the equations of motion can be written with the aid of Lagrange's equation in the form

$$\frac{d}{dt}\left(\frac{\partial T}{\partial \dot{\xi}_i}\right) - \frac{\partial T}{\partial \xi_i} + \frac{\partial U}{\partial \xi_i} + \frac{\partial F}{\partial \dot{\xi}_i} = Q_i \tag{2}$$

where T and U are the kinetic and potential energies, respectively, F is a dissipation function, and Q_i is a generalized force.

Kinetic and potential energies.- The kinetic and potential energies of the system can be determined by using the properties of normal modes. The kinetic energy will be

$$T = \frac{1}{2} \iint_S m(x',y')\left[\dot{z}(x',y',t)\right]^2 dx'\, dy' \tag{3}$$

where S denotes integration over the entire surface of the wing. Combining equation (1) with equation (3) yields

$$T = \frac{1}{2} \sum_{i=1}^{I} \sum_{j=1}^{I} \dot{\xi}_i(t)\dot{\xi}_j(t) \iint_S m(x',y')\left[f_i(x',y')\right]\left[f_j(x',y')\right] dx'\, dy' \tag{4}$$

Since the modal functions are normal modes, the orthogonality relation, derived, for example, in reference 4, applies. That is,

$$\left.\begin{aligned} \iint_S m(x',y')\left[f_i(x',y')\right]\left[f_j(x',y')\right]dx'\ dy' &= M_i \qquad (i = j) \\ \iint_S m(x',y')\left[f_i(x',y')\right]\left[f_j(x',y')\right]dx'\ dy' &= 0 \qquad (i \neq j) \end{aligned}\right\} \tag{5}$$

where M_i is the generalized mass in mode i. Thus, the kinetic energy can be written by using equation (5) as

$$T = \frac{1}{2}\sum_{i=1}^{I} M_i\left[\dot{\xi}_i(t)\right]^2 \tag{6}$$

The potential energy of the system is

$$U = \frac{1}{2}\iint_S k(x',y')\left[z(x',y',t)\right]^2 dx'\ dy' \tag{7}$$

Substituting equation (1) into equation (7) yields

$$U = \frac{1}{2}\sum_{i=1}^{I}\sum_{j=1}^{I}\xi_i(t)\xi_j(t)\iint_S k(x',y')\left[f_i(x',y')\right]\left[f_j(x',y')\right]dx'\ dy' \tag{8}$$

Now, the orthogonality relation of equation (5) can be written as

$$\left.\begin{aligned} \iint_S k(x',y')\left[f_i(x',y')\right]\left[f_j(x',y')\right]dx'\ dy' &= \omega_i^2 M_i \qquad (i = j) \\ \iint_S k(x',y')\left[f_i(x',y')\right]\left[f_j(x',y')\right]dx'\ dy' &= 0 \qquad (i \neq j) \end{aligned}\right\} \tag{9}$$

where ω_i is the natural frequency of mode i. Thus, the potential energy is

$$U = \frac{1}{2}\sum_{i=1}^{I}\omega_i^2 M_i\left[\xi_i(t)\right]^2 \tag{10}$$

Dissipation function.- Reference 5 discusses the development of a dissipation function which is convenient for allowing for internal damping in flutter analyses for the particular case of harmonic time variation. This function is a convenient expression which, when differentiated with respect to the velocities $\dot{\xi}_i(t)$, gives the generalized damping force in the system. For a wing which has structural damping, the dissipation function can be written

$$F = \frac{1}{2} \sum_{i=1}^{I} g_i M_i \frac{\omega_i^2}{\omega} \left[\dot{\xi}_i(t)\right]^2 \tag{11}$$

where g_i is the structural damping coefficient in mode i.

Equations of motion.- Operating on equations (6), (10), and (11), as indicated by equation (2), yields the equations of motion

$$M_i \ddot{\xi}_i(t) + g_i M_i \frac{\omega_i^2}{\omega} \dot{\xi}_i(t) + \omega_i^2 M_i \xi_i(t) = \sum_{j=1}^{I} Q_j \tag{12}$$

Generalized Forces

The external forces acting on the wing which influence the flutter system are aerodynamic forces. These aerodynamic forces will be calculated by two procedures: (a) piston theory and (b) a quasi-steady method based on second-order two-dimensional theory.

Piston theory.- Piston theory has been developed and discussed in references 1 to 3. The basic assumptions of this theory are slender profiles and high Mach numbers $(M^2 \gg 1.0)$. As a result of these assumptions, the x' component of fluid velocity changes very little along the profile and is always much greater than the speed of sound. This means that disturbances at one point on the wing induce only a small effect at another point. Piston theory neglects these small induced effects by assuming a point function relation between pressure and downwash velocity. This relation assumes that the local pressure on an airfoil is related to the local fluid velocity normal to the free stream in the same manner that the pressure on a piston in a one-dimensional channel is related to the velocity of the piston. Obviously, three-dimensional effects are not included in piston theory. However, these effects on wings are relatively small at high flight speeds.

The second-order piston-theory relation between pressure and downwash, as given in reference 3, is

$$p - p_\infty = \rho a^2\left[\frac{w}{a} + \frac{\gamma + 1}{4}\left(\frac{w}{a}\right)^2\right] \tag{13}$$

The downwash (or piston velocity) at the point under consideration is w and w/a should be less than 1.0. This expression has been found to apply reasonably well for Mach numbers greater than about 2.0.

Quasi-steady second-order theory.- An expression similar to piston theory for the pressure on a wing can be obtained from the second-order theory for steady flow which is given, for instance, in reference 6. If the local steady angle of attack at a point on the surface is replaced by the instantaneous (slowly varying, hence quasi-steady) local angle of attack, the pressure at the point is

$$p - p_\infty = \rho a^2\left(\frac{M}{\beta}\right)\left[\frac{w}{a} + \frac{M^4(\gamma + 1) - 4\beta^2}{4\beta^3 M}\left(\frac{w}{a}\right)^2\right] \tag{14}$$

Equation (14) approaches the piston-theory pressure (eq. (13)) if the Mach number is very large; that is, $\beta \approx M$. Equation (14) contains no assumption about the Mach number being large; this expression could give more useful results for pressure than piston theory in a range of Mach numbers around 2.0.

Downwash.- The downwash appearing in equations (13) and (14) is the instantaneous local slope in the stream direction multiplied by the free-stream velocity. It can be separated into displacement and airfoil-shape terms (as in ref. 2) which are not the same for the upper and lower surfaces of the wing. If $z(x',y',t)$ is the position of the mean surface and $Z(x',y')$ describes the contour of the airfoil surface measured from the mean surface, the downwash will be

For the upper surface:

$$w = \left(V\frac{\partial}{\partial x'} + \frac{\partial}{\partial t}\right)z(x',y',t) + V\frac{\partial Z(x',y')}{\partial x'} \tag{15a}$$

For the lower surface:

$$w = -\left(V\frac{\partial}{\partial x'} + \frac{\partial}{\partial t}\right)z(x',y',t) + V\frac{\partial Z(x',y')}{\partial x'} \tag{15b}$$

Downwash is positive when measured away from the surface of the wing.

Differential pressures.- Pressures acting on the wing surface are found by substituting equation (15) into equation (13) or (14). The

differential pressure, in the positive z' direction, acting across the wing is then determined by subtracting the pressure on the upper surface from the pressure on the lower surface. If only time-dependent terms and terms which are linear in displacement are retained, the differential pressure when the piston theory is used is

$$\Delta p(x',y',t) = -2\rho a\left[1 + G\frac{\partial}{\partial x'}Z(x',y')\right]\left[\left(V\frac{\partial}{\partial x'} + \frac{\partial}{\partial t}\right)z(x',y',t)\right] \quad (16)$$

where $G = M\frac{\gamma + 1}{2}$. Use of the quasi-steady theory would multiply the right-hand side of equation (16) by a factor of M/β and change the factor G to $\bar{G} = \frac{M^4(\gamma + 1) - 4\beta^2}{2\beta^3}$. The factor $\bar{G}$ approaches G for very large Mach numbers.

The modal representation of the wing's motion (eq. (1)) can be substituted into equation (16) and the resulting expression for the differential pressure is

$$\Delta p(x',y',t) = -2\rho a\sum_{j=1}^{I}\left[1 + G\frac{\partial}{\partial x'}Z(x',y')\right]\left[V\frac{\partial f_j(x',y')}{\partial x'}\xi_j(t) + f_j(x',y')\dot{\xi}_j(t)\right] \quad (17)$$

Generalized aerodynamic forces.- The generalized aerodynamic force in mode i can be interpreted in terms of the total virtual work in mode i due to the aerodynamic forces. As shown in reference 4, this generalized force is determined by the integration over the surface of the product of the differential pressure distribution and the deflection distribution in mode i. The result for piston theory, when equation (17) is used for the pressure, is

$$Q_i = -2\rho a\sum_{j=1}^{I}\iint_S\left[1 + G\frac{\partial}{\partial x'}Z(x',y')\right]\left[V\frac{\partial f_j(x',y')}{\partial x'}\xi_j(t) + f_j(x',y')\dot{\xi}_j(t)\right]\left[f_i(x',y')\right]dx'\,dy' \quad (18)$$

For systematic evaluation of equation (18), it is convenient to separate the terms as follows:

$$Q_i = -2\rho a \sum_{j=1}^{I} \left[V\left(A_{ij} + GC_{ij}\right)\xi_j(t) + \left(B_{ij} + GD_{ij}\right)\dot{\xi}_j(t) \right] \tag{19}$$

where

$$\left.\begin{aligned} A_{ij} &= \iint_S \left[\frac{\partial f_j(x',y')}{\partial x'}\right]\left[f_i(x',y')\right] dx'\, dy' \\ B_{ij} &= \iint_S \left[f_j(x',y')\right]\left[f_i(x',y')\right] dx'\, dy' \\ C_{ij} &= \iint_S \left[\frac{\partial}{\partial x'} Z(x',y')\right]\left[\frac{\partial f_j(x',y')}{\partial x'}\right]\left[f_i(x',y')\right] dx'\, dy' \\ D_{ij} &= \iint_S \left[\frac{\partial}{\partial x'} Z(x',y')\right]\left[f_j(x',y')\right]\left[f_i(x',y')\right] dx'\, dy' \end{aligned}\right\} \tag{20}$$

Equations (20) are parameters which are constant for a given wing, depending only on the mode shape and the contour of the wing surface. The quasi-steady aerodynamic theory will alter the generalized force expression (eq. (19)) by the multiplicative factor M/β and substitute $\bar{G}$ for G.

Flutter Determinant

The flutter determinant for this system may be obtained from the equations of motion (eq. (12)) and the generalized forces (eq. (19)). In order to obtain a flutter solution, the assumption is made that the damping coefficient in all modes is the same; that is, $g_1 = g_2 = \ldots = g$. The assumption of simple harmonic motion is not required when the simplified aerodynamic theories are used since the roots of the characteristic equation could be examined directly. However, this procedure is presented in the usual form for flutter calculations by letting the time variation be a simple harmonic variation to obtain the borderline flutter condition. If equations (12) and (19) are combined and the terms rearranged, the equations of motion at flutter for piston-theory aerodynamics become

$$M_1\left[\left(\frac{\omega_1}{\omega_1}\right)^2 X - 1\right]\bar{\xi}_1 + \frac{2\rho}{M}\sum_{j=1}^{I}\left[\left(\frac{b_R}{k_R}\right)^2\left(A_{ij} + GC_{ij}\right) + i\left(\frac{b_R}{k_R}\right)\left(B_{ij} + GD_{ij}\right)\right]\bar{\xi}_j = 0 \qquad \text{(subscript } i = 1, 2, \ldots I\text{)} \quad (21)$$

where

$$\left.\begin{aligned} \xi(t) &= \bar{\xi}e^{i\omega t} \\ X &= \left(\frac{\omega_1}{\omega}\right)^2(1 + ig) \\ k_R &= b_R\frac{\omega}{V} \end{aligned}\right\} \quad (22)$$

The subscript R refers to any convenient reference station.

The requirement for a nontrivial solution to equations (21) is that the determinant of the coefficients of $\bar{\xi}_i$ must vanish. Thus, in matrix notation,

$$\left|\frac{M}{2\rho}\left[M_1\left(X\left(\frac{\omega_1}{\omega_1}\right)^2 - 1\right)\right] + \left(\frac{b_R}{k_R}\right)^2\left[A_{ij} + GC_{ij}\right] + i\left(\frac{b_R}{k_R}\right)\left[B_{ij} + GD_{ij}\right]\right| = 0 \quad (23)$$

where $[\ ]$ indicates a square matrix and $\left[\searrow\right]$ indicates a diagonal matrix. This equation must be satisfied at any reduced frequency, Mach number, and density as long as the motion is simple harmonic. A common method of finding the borderline case of neutral stability is by solving for the velocity at which zero damping is required to maintain harmonic motion.

This flutter determinant has been derived by using piston-theory aerodynamics. If the quasi-steady pressures given by equation (14) had been used, the flutter determinant would be the same except that β would replace M and the factor G would be replaced by $\bar{G}$.

The flutter equations as derived herein contain airfoil-shape terms. The usual assumption of linearized supersonic theory is that these terms are negligible. In order to drop thickness terms from this calculation and thus have a high Mach number low-frequency approximation for linear theory, it is only necessary to set the factor G (or $\bar{G}$) equal to zero wherever it appears in the flutter determinant.

Representation of Wing Deflections

Closed-form evaluation of the surface integrals defined by equations (5) and (20) is not practical for the complex modal deformation shapes normally possessed by wings. In this report, a numerical evaluation of these integrals is accomplished by approximating the wing characteristics at a limited number of spanwise stations, performing the chordwise integrations, and then summing spanwise. In order to use this method, the wing is divided into N spanwise stations, parallel to the airstream. At each of these stations, the chordwise distribution of displacement in mode i is approximated by a polynomial of degree P over the chord ahead of the flap and by a polynomial of degree Q over the flap, as shown in figure 1. That is, the total deflection at station n in mode i is given by

$$\left.\begin{aligned} f_i^{(n)}(x) &= \sum_{p=0}^{P} \left(a_i^{(n)}\right)_p x^p \qquad \left(0 \leqq x \leqq x_1\right) \\ f_i^{(n)}(x) &= \sum_{q=0}^{Q} \left(b_i^{(n)}\right)_q x^q \qquad \left(x_1 \leqq x \leqq 1.0\right) \end{aligned}\right\} \tag{24}$$

where x is a nondimensional streamwise coordinate having the value zero at the leading edge and 1.0 at the trailing edge. The coefficients $\left(a_i^{(n)}\right)_p$ and $\left(b_i^{(n)}\right)_q$ are constants. This series of equations approximates the modal function $f_i(x',y')$ where the y' variation has been replaced by an approximation at N spanwise stations, denoted by the index n.

The surface integrals of equation (20) can be written in terms of the deflection polynomials by substituting equation (24). The integrals of equation (20) involve the products of two polynomials or the product of a polynomial and the derivative of another polynomial. The spanwise coordinate becomes y, which is zero at the wing root and unity at the tip. The chordwise integrations for C_{ij} and D_{ij} are done by parts in order to get the airfoil cross-sectional properties in convenient form. Thus, equations (20) become

$$
\left.
\begin{aligned}
A_{ij} &= l\int_0^1 \left\{ \int_0^{x_1} \left[\sum_{p=0}^{P_j} \sum_{r=0}^{P_i} p\left(a_j^{(n)}\right)_p \left(a_i^{(n)}\right)_r x^{p+r-1} \right] dx + \int_{x_1}^{1.0} \left[\sum_{q=0}^{Q_j} \sum_{s=0}^{Q_i} q\left(b_j^{(n)}\right)_q \left(b_i^{(n)}\right)_s x^{q+s-1} \right] dx \right\} dy \\
B_{ij} &= 2b_R l\int_0^1 \frac{b}{b_R} \left\{ \int_0^{x_1} \left[\sum_{p=0}^{P_j} \sum_{r=0}^{P_i} \left(a_j^{(n)}\right)_p \left(a_i^{(n)}\right)_r x^{p+r} \right] dx + \int_{x_1}^{1.0} \left[\sum_{q=0}^{Q_j} \sum_{s=0}^{Q_i} \left(b_j^{(n)}\right)_q \left(b_i^{(n)}\right)_s x^{q+s} \right] dx \right\} dy \\
C_{ij} &= l\int_0^1 \left[\sum_{p=0}^{P_j} \sum_{r=0}^{P_i} p\left(a_j^{(n)}\right)_p \left(a_i^{(n)}\right)_r \left(t_{p+r-1}^{(n)}\right) + \sum_{q=0}^{Q_j} \sum_{s=0}^{Q_i} q\left(b_j^{(n)}\right)_q \left(\overline{b_i^{(n)}}\right)_s \left(s_{q+s-1}^{(n)}\right) \right] dy \\
D_{ij} &= 2b_R l\int_0^1 \frac{b}{b_R} \left[\sum_{p=0}^{P_j} \sum_{r=0}^{P_i} \left(a_j^{(n)}\right)_p \left(a_i^{(n)}\right)_R \left(t_{p+r}^{(n)}\right) + \sum_{q=0}^{Q_j} \sum_{r=0}^{Q_i} \left(b_j^{(n)}\right)_q \left(b_i^{(n)}\right)_s \left(s_{q+s}^{(n)}\right) \right] dy
\end{aligned}
\right\} \quad (25)
$$

The $t_\nu^{(n)}$ and $s_\nu^{(n)}$ terms appearing in these equations are constants which are determined by the airfoil thickness and cross section and are defined by the following equations:

$$
\left.
\begin{aligned}
t_\nu^{(n)} &= \left(x_1\right)^\nu \left[\frac{Z^{(n)}(x_1)}{2b} \right] - \nu \int_0^{x_1} x^{\nu-1} \left[\frac{Z^{(n)}(x)}{2b} \right] dx \\
s_\nu^{(n)} &= \left[\frac{Z^{(n)}(1)}{2b} \right] - \left(x_1\right)^\nu \left[\frac{Z^{(n)}(x_1)}{2b} \right] - \nu \int_{x_1}^1 x^{\nu-1} \left[\frac{Z^{(n)}(x)}{2b} \right] dx
\end{aligned}
\right\} \quad (26)
$$

where ν takes on the values of the indices in equation (25). The quantity $Z^{(n)}(x)$, illustrated in figure 2, describes the airfoil contour at station n and is taken as positive when measured away from the mean chord.

When the thickness goes to zero, the $t_\nu^{(n)}$ and $s_\nu^{(n)}$ terms become zero. However, as previously mentioned, a zero-thickness calculation can be accomplished numerically by setting G or $\bar{G}$ equal to zero.

Generalized Mass

Distributed mass.- The generalized mass M_i (defined by eq. (5)) can be computed in any convenient manner. However, if the wing is of solid construction or has a mass distribution which is not too irregular, the mass distribution can be approximated at the N stations discussed in a previous section by a series of parabolas; thus the generalized mass can easily be evaluated. If the wing chord at a spanwise station n is broken into K arbitrary intervals, as shown in figure 3, the mass per unit area in any one of the intervals κ is given by

$$m^{(n)}(x) = \left(m_0^{(n)}\right)_\kappa + \left(m_1^{(n)}\right)_\kappa x + \left(m_2^{(n)}\right)_\kappa x^2 \qquad \left(l_{\kappa-1} \leqq x \leqq l_\kappa\right) \tag{27}$$

If the wing has an aileron, the appropriate mass interval can be made to coincide with the aileron. That is, l_{K-1} will equal x_1 for the example illustrated. With the mass distribution approximated in this manner and the deflections approximated by equation (24), the generalized mass from equation (5) becomes

$$M_i = 2b_R l \int_0^1 \frac{b}{b_R} \left\{ \sum_{\kappa=1}^{K-1} \int_{l_{\kappa-1}}^{l_\kappa} \left[\left(m_0^{(n)}\right)_\kappa + \left(m_1^{(n)}\right)_\kappa x + \left(m_2^{(n)}\right)_\kappa x^2 \right] \left[\sum_{p=0}^{P} \left(a_i^{(n)}\right)_p x^p \right]^2 dx + \int_{l_{K-1}}^{1.0} \left[\left(m_0^{(n)}\right)_K + \left(m_1^{(n)}\right)_K x + \left(m_2^{(n)}\right)_K x^2 \right] \left[\sum_{q=0}^{Q} \left(b_i^{(n)}\right)_q x^q \right]^2 dx \right\} dy \tag{28}$$

External stores and pods.- In order to account for rigidly attached external stores or pods, additions must be made to the previous analysis. For the present case, the assumption is made that aerodynamic forces acting on the body are negligible. This means that the terms A_{ij}, B_{ij}, C_{ij}, and D_{ij} defined by equation (20) are unaffected. The only way that the stores can enter the problem is through the kinetic and potential energies and the dissipation function.

If the store is represented by a concentrated mass, inertia, and unbalance about its attachment point, the attachment point displacement and slope in the stream direction for mode i being given by δ_i and ϵ_i, respectively, the increment in kinetic energy which must be added to equation (4) is

$$\Delta T = \frac{1}{2} \sum_{i=1}^{I} \sum_{j=1}^{I} \dot{\xi}_i(t)\dot{\xi}_j(t)\left[m_s\delta_i\delta_j + S_{\alpha_s}\left(\epsilon_i\delta_j + \epsilon_j\delta_i\right) + I_{\alpha_s}\epsilon_i\epsilon_j\right] \tag{29}$$

The orthogonality relation between normal modes will apply for modes determined with the additional mass of the store in the system. Thus, the generalized mass M_i for a wing carrying external stores would be

$$M_i = \iint_S m(x',y')\left[f_i(x',y')\right]^2 dx'\,dy' + \left[m_s\delta_i^2 + 2S_{\alpha_s}\epsilon_i\delta_i + I_{\alpha_s}\epsilon_i^2\right] \tag{30}$$

With this new definition of the generalized mass, the kinetic and potential energies and the dissipation function appear as before in equations (6), (10), and (11). Therefore, if a wing is carrying stores, the generalized mass given by equation (28) must be increased by an increment

$$\Delta M_i = m_s\delta_i^2 + 2S_{\alpha_s}\delta_i\epsilon_i + I_{\alpha_s}\epsilon_i^2 \tag{31}$$

This is the mass effect of the store. If the aerodynamic forces are known, they can be included along with the other aerodynamic terms.

APPLICATION AND COMPARISON WITH EXPERIMENT

The method described in the previous section has been used to calculate the flutter characteristics of several cantilevered wings at supersonic speeds. Typical results of these calculations and comparisons with experiment will be presented for three wings. Piston-theory calculations for Mach numbers as low as 1.3 were made for comparison with experiment and with quasi-steady theory, although the piston-theory region of applicability is usually considered to be Mach numbers greater than about 2.

Two of the wings covered by these calculations were 60° and 45° flat-plate delta wings. Their airfoil sections were flat with a slight bevel at the leading edge and were approximately 0.5 percent thick at the root. A third wing studied was a uniform untapered 45° swept wing with a panel aspect ratio of 1.33. Its airfoil section was flat sided with both edges beveled and was 1.4 percent thick. The geometric, mass, and vibration characteristics of these wings are given in reference 7. Their experimental flutter characteristics were reported in reference 8.

Approximation of Wing Properties

For the wings under consideration, the experimentally determined camber mode shapes from reference 7 were approximated by linear, quadratic, and cubic polynomials. Thus, the maximum value of P from equation (24) was 3. None of the wings had flaps; thus x_1 in equation (1) may be set equal to 1.0. The accuracy of the approximation for camber mode shapes is illustrated in figure 4 where the camber modes and their polynomial approximations are plotted at various span stations for the first three vibration modes of the 45° delta wing. Figure 4 also shows the large amount of camber deformation present in wings of this type. The approximations are seen to be best near the tip where the deflections are the greatest. Also, the approximations are better in the lower modes (figs. 4(a) and 4(b)) than in the third mode (fig. 4(c)). Better approximations in the higher modes could probably be obtained by using polynomials of higher degree.

For this group of wings, ten spanwise stations ($N = 10$) at 95-, 85-, 75-, . . . 5-percent span were chosen for computing the system properties. Spanwise integrations were made by using a ten-point numerical integration scheme.

The 60° and 45° flat-plate delta wings had constant mass distributions, the bevel being neglected. The 45° swept wing was a plate with beveled edges such that the mass distribution was proportional to the thickness at any point. The chordwise mass distribution was constant over the center portion of the chord and had a linear variation over the beveled edges. Equation (27) described this distribution accurately with $K = 3$.

Results of Flutter Calculations on Flat-Plate Delta Wings

The calculations on one wing, the 60° flat-plate delta, are fully described in the appendix. The results are shown in figure 5 and compared with experiment from reference 8. Four separate results of this three-mode calculation are shown: for piston theory with and without the airfoil-thickness term and for quasi-steady theory with and without

the thickness term. The flutter frequencies, shown as ratios to the lowest natural frequency, are calculated by all methods to within 15 percent for Mach numbers from 1.3 to 3.0. The flutter boundary is shown in figure 5 as a plot of the stiffness-altitude parameter $\frac{b\omega_2}{a}\sqrt{\mu}$ against Mach number.

The stiffness-altitude parameter, used in figure 5 and subsequent figures, depends only upon the physical properties of the wing (in particular, the stiffness) and upon the atmosphere in which it operates. Its value increases as either the altitude or the stiffness increases. When plotted as the ordinate against Mach number, as in these figures, constant dynamic pressure curves will appear as radial lines through the origin. The stable region will be above the flutter boundary.

In this case, piston theory predicts flutter on the conservative side within 23 percent of experiment at $M = 1.3$ and within 9 percent at $M = 3.0$. Quasi-steady theory predicts flutter still more conservatively, within 45 percent at $M = 1.3$ and within 12 percent at $M = 3.0$. In both instances, as would be expected for a thin, flat-plate wing, thickness terms in the aerodynamic theory had very little effect. It should be noted that, on a percentage basis, both theories give better agreement with experiment as the Mach number becomes larger and the reduced frequency becomes smaller.

The results of similar three-mode calculations on a 45° flat-plate delta wing are shown in figure 6. The experimental data are from reference 8. Agreement between calculation and experiment is better than that for the 60° delta wing but the calculations are now slightly unconservative. Piston theory deviated from experiment by 14 percent at $M = 1.3$ and by 3 percent at $M = 3$; thus, the accuracy improved as the Mach number increased. Quasi-steady theory showed better agreement than piston theory in this case, 2 percent at $M = 1.3$ and $M = 3$. Again, thickness terms in the aerodynamic theory had very little effect on the calculated flutter speed. Calculated flutter frequency was good, within 6 percent at all Mach numbers.

Results of Flutter Calculations on a Flat-Plate 45° Swept Wing

The results of calculations made with three modes on the untapered 45° swept wing are shown in figure 7. Agreement with experimental data from reference 8 is not nearly as good as that for the delta wings. The calculated flutter frequency is seen to be high by about 95 percent for all four methods of calculation. The flutter boundary is predicted unconservatively by all methods. A possible explanation for the sizable discrepancy between calculations and experiment is the large tip effect.

Especially at lower Mach numbers, this wing will have a large portion of its surface influenced by the tip, which is parallel to the flow. This effect was not present on the delta wings.

CONCLUDING REMARKS

A high supersonic Mach number flutter-calculation procedure for wings with camber in their vibration modes has been described. The normal (coupled) vibration modes of the wing are utilized and their camber deflections are approximated by polynomials. The wing may have a control surface and may carry external stores. Aerodynamic forces on the stores are neglected but could be included if desired. The aerodynamic forces acting on the wing are obtained from piston theory and also by a quasi-steady method based on second-order supersonic theory. Both aerodynamic theories allow airfoil shape and thickness terms to be included. Use of the piston theory requires the Mach number squared to be much greater than 1 and both aerodynamic theories require the reduced frequency to be low.

The method was used to calculate the flutter speed of three cantilevered wings from Mach numbers of 1.3 to 3.0. Good agreement with experiment was found for a 60° and a 45° flat-plate delta wing. Sizable differences from experiment resulted when the method was applied to an untapered 45° swept wing.

Langley Aeronautical Laboratory,
National Advisory Committee for Aeronautics,
Langley Field, Va., August 8, 1958.

APPENDIX

SAMPLE CALCULATIONS ON A 60° FLAT-PLATE DELTA WING

The method of flutter calculations described in the body of the paper is illustrated here for the 60° flat-plate delta wing. The wing was made of a flat plate of metal and was cantilever mounted at the root. All computations were performed on digital computers.

The modal data needed in the calculation are given in table I. The first three vibration modes are used and the wing deflections are determined at ten spanwise stations. In order to specify the chordwise polynomial for each vibration mode and at each station n, the degree of the polynomial P and the coordinates of the polynomial at $P + 1$ chordwise points are given. Then, by solving a set of $P + 1$ simultaneous equations, the constants of equation (24) can be evaluated for each station n and each vibration mode.

With the constants of the deflection polynomials determined, the flutter-determinant elements given by equations (25) and (28) can be evaluated by using the mass and geometric data given in table I. Note that for this flat-plate wing the mass distribution is constant. The airfoil has been assumed to have zero thickness at the leading edge, flat sides, and nonzero thickness at the trailing edge; thus all thickness terms are zero except $t_0^{(n)}$. The wing does not have a flap so the x_1 dimension is set equal to 1.0. The elements for the flutter determinant computed by using this data are

$$\left[M_1\right] = 10^{-4}\begin{bmatrix} 1.1087469 & 0 & 0 \\ 0 & 2.2970845 & 0 \\ 0 & 0 & 0.92344991 \end{bmatrix}$$

$$
\left.
\begin{aligned}
b_R^2\left[A_{ij}\right] &= 10^{-2}\begin{bmatrix} 0.24745638 & 1.7161381 & -0.47849789 \\ -0.24950129 & -0.15541714 & 0.34179249 \\ 0.068579763 & -0.24973402 & 0.20163600 \end{bmatrix} \\
b_R\left[B_{ij}\right] &= 10^{-3}\begin{bmatrix} 3.9726354 & -0.24698912 & -0.14509758 \\ -0.24698926 & 8.2304250 & 0.071423468 \\ -0.14509758 & 0.071423539 & 3.3087173 \end{bmatrix} \\
b_R^2\left[C_{ij}\right] &= 10^{-4}\begin{bmatrix} 0.50658132 & 1.1599243 & -0.014184357 \\ -0.25845494 & 1.2900028 & -0.34968308 \\ 0.42135938 & 1.1803951 & -0.037120715 \end{bmatrix} \\
b_R\left[D_{ij}\right] &= 10^{-5}\begin{bmatrix} 3.1259500 & -0.50451053 & 2.7703439 \\ -0.50451053 & 6.9119095 & 0.54545789 \\ 2.7703439 & 0.54545789 & 2.6712828 \end{bmatrix}
\end{aligned}
\right\} \quad \text{(A1)}
$$

These elements, computed from equations (25) and (28), together with the natural frequencies, are fixed for this wing. The aerodynamic parameters, Mach number and density, can be varied independently in the flutter determinant of equation (23). For example, if the wing fluttered at a density of 0.00063 slug/cu ft at Mach number 3.0, the factor G is 3.6 and the flutter determinant is

$$\begin{vmatrix} 0.86398756(X-1) + 0.0026965551\left(\frac{1}{k_R^2}\right) + 0.0040851696\left(\frac{1}{k_R}\right) & 0.01578574\left(\frac{1}{k_R^2}\right) - 0.00086515850\left(\frac{1}{k_R}\right) & -0.0047900853\left(\frac{1}{k_R^2}\right) - 0.000045565200\left(\frac{1}{k_R}\right) \\ -0.0085880567\left(\frac{1}{k_R^2}\right) - 0.00084505164\left(\frac{1}{k_R}\right) & 4.5594766X - 0.5469488 - 0.0010897705\left(\frac{1}{k_R^2}\right) + 0.0084792557\left(\frac{1}{k_R}\right) & 0.0058980590\left(\frac{1}{k_R^2}\right) + 0.000091079852\left(\frac{1}{k_R}\right) \\ 0.00085746701\left(\frac{1}{k_R^2}\right) - 0.00047565800\left(\frac{1}{k_R}\right) & -0.0080719980\left(\frac{1}{k_R^2}\right) + 0.000091060085\left(\frac{1}{k_R}\right) & 3.7567817X - 0.01986508 + 0.0080028965\left(\frac{1}{k_R^2}\right) + 0.0054048855\left(\frac{1}{k_R}\right) \end{vmatrix} = 0 \quad \text{(A8)}$$

This complex determinant can be solved for flutter speed and frequency in a number of ways. The most common method is to substitute successive reduced frequencies k_R and to solve each time for the complex root X, defined by equation (22). At flutter the imaginary part of this root, proportional to the damping required to produce harmonic motion, is zero. Plots of damping coefficient and frequency obtained in this manner are shown in figure 8. From this figure it is seen that the root corresponding to the second natural vibration mode becomes unstable at $\frac{1}{k} = 53$ and a frequency which is 2.33 times the first natural frequency. Thus, the flutter frequency is 156 cps and the flutter velocity is 1,842 ft/sec. This result is plotted in figure 5.

If it were desired to use quasi-steady aerodynamics at the same Mach number, $\beta = 2.83$ would be substituted for M and $\bar{G} = 3.58$ for G in equation (23). The terms G or $\bar{G}$ can be set equal to zero for a zero-thickness calculation.

REFERENCES

1. Morgan, Homer G., Runyan, Harry L., and Huckel, Vera: Theoretical Considerations of Flutter at High Mach Numbers. Jour. Aero. Sci., vol. 25, no. 6, June 1958, pp. 371-381.

2. Lighthill, M. J.: Oscillating Airfoils at High Mach Number. Jour. Aero. Sci., vol. 20, no. 6, June 1953, pp. 402-406.

3. Ashley, Holt, and Zartarian, Garabed: Piston Theory - A New Aerodynamic Tool for the Aeroelastician. Jour. Aero. Sci., vol. 23, no. 12, Dec. 1956, pp. 1109-1118.

4. Bisplinghoff, Raymond L., Ashley, Holt, and Halfman, Robert L.: Aeroelasticity. Addison-Wesley Pub. Co., Inc. (Cambridge, Mass.), c.1955.

5. Scanlan, Robert H., and Rosenbaum, Robert: Introduction to the Study of Aircraft Vibration and Flutter. The MacMillan Co., 1951.

6. Van Dyke, Milton D.: A Study of Second-Order Supersonic Flow Theory. NACA Rep. 1081, 1952. (Supersedes NACA TN 2200.)

7. Hanson, Perry W., and Tuovila, W. J.: Experimentally Determined Natural Vibration Modes of Some Cantilever-Wing Flutter Models by Using an Acceleration Method. NACA TN 4010, 1957.

8. Tuovila, W. J., and McCarty, John Locke: Experimental Flutter Results for Cantilever-Wing Models at Mach Numbers up to 3.0. NACA RM L55E11, 1955.

TABLE I

MASS, MODAL, AND GEOMETRIC DATA FOR FLUTTER CALCULATIONS IN THE APPENDIX

Vibration mode	n = 1		n = 2		n = 3		n = 4		n = 5		n = 6		n = 7		n = 8		n = 9		n = 10	
	x	$f_1^{(1)}$	x	$f_1^{(2)}$	x	$f_1^{(3)}$	x	$f_1^{(4)}$	x	$f_1^{(5)}$	x	$f_1^{(6)}$	x	$f_1^{(7)}$	x	$f_1^{(8)}$	x	$f_1^{(9)}$	x	$f_1^{(10)}$
1	P = 2		P = 2		P = 2		P = 2		P = 2		P = 2		P = 3		P = 3		P = 3		P = 2	
	0	0.870	0	0.641	0	0.447	0	0.300	0	0.185	0	0.097	0	0.043	0	0.017	0	0.006	0	0.001
	.5	.915	.5	.736	.5	.611	.5	.476	.5	.354	.5	.248	.25	.097	.25	.045	.25	.017	.5	.005
	1.0	.932	1.0	.788	1.0	.649	1.0	.518	1.0	.397	1.0	.290	.75	.198	.75	.120	.75	.052	1.0	.006
													1.0	.198	1.0	.120	1.0	.052		
2	P = 2		P = 3		P = 3		P = 3		P = 3		P = 3		P = 3		P = 3		P = 2		P = 2	
	0	0.650	0	-0.055	0	-0.632	0	-0.930	0	-0.920	0	-0.735	0	-0.448	0	-0.175	0	-0.053	0	-0.008
	.5	.820	.25	.213	.25	-.300	.25	-.745	.25	-.985	.25	-.690	.25	-.605	.25	-.365	.5	-.179	.5	-.050
	1.0	.935	.75	.670	.75	.467	.75	.270	.50	-.420	.50	-.445	.50	-.383	.50	-.300	1.0	.077	1.0	.019
			1.0	.810	1.0	.690	1.0	.570	1.0	.455	1.0	.347	1.0	.245	1.0	.153				
3	P = 2		P = 2		P = 3		P = 3		P = 3		P = 3		P = 3		P = 3		P = 3		P = 2	
	0	0.918	0	0.572	0	0.278	0	0.053	0	0.021	0	0.075	0	0.089	0	0.055	0	0.020	0	0.002
	.5	.897	.5	.322	.25	.257	.25	.055	.25	-.015	.25	.048	.25	.078	.25	.072	.25	.045	.25	.090
	1.0	.882	1.0	.420	.75	.116	.75	-.180	.75	-.405	.75	-.326	.75	-.490	.75	-.326	.75	-.144	1.0	-.050
					1.0	.045	1.0	-.244	1.0	-.448	1.0	-.568	1.0	-.542	1.0	-.435	1.0	-.256		

Station n	y'/l	b/b_R	$t_0^{(n)}$
1	0.95	0.05	0.08010
2	.85	.15	.02670
3	.75	.25	.01602
4	.65	.35	.01144
5	.55	.45	.00890
6	.45	.55	.00728
7	.35	.65	.00616
8	.25	.75	.00534
9	.15	.85	.00471
10	.05	.95	.00421

$t_1^{(n)} = t_2^{(n)} = t_3^{(n)} = \ldots = 0$

$\left(m_0^{(n)}\right)_x = 0.00988$ lb-sec^2/ft/ft^2

$\left(m_1^{(n)}\right)_x = \left(m_2^{(n)}\right)_x = 0$

$x_1 = 1.0$

$b_R = 0.354$ ft

$l = 0.409$ ft

$\omega_1 = 421$ radians/sec

$\left(\frac{\omega_2}{\omega_1}\right)^2 = 8.30$

$\left(\frac{\omega_3}{\omega_1}\right)^2 = 26.1$

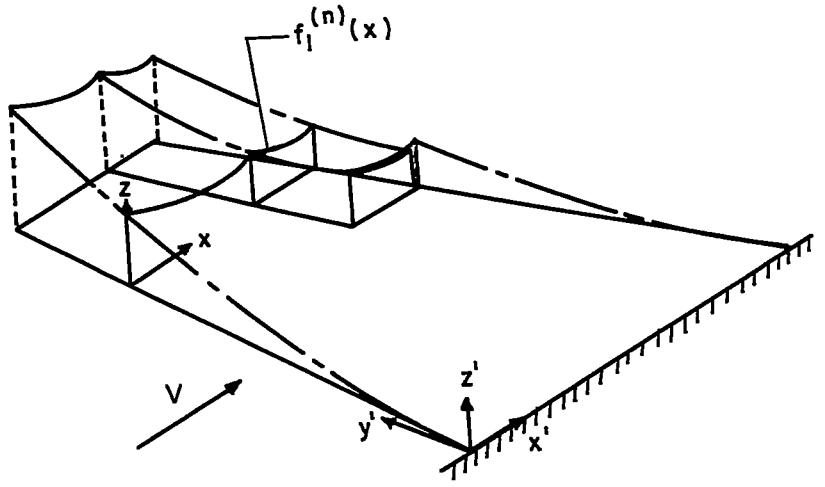

Figure 1.- Schematic drawing showing the wing deflection for a single mode.

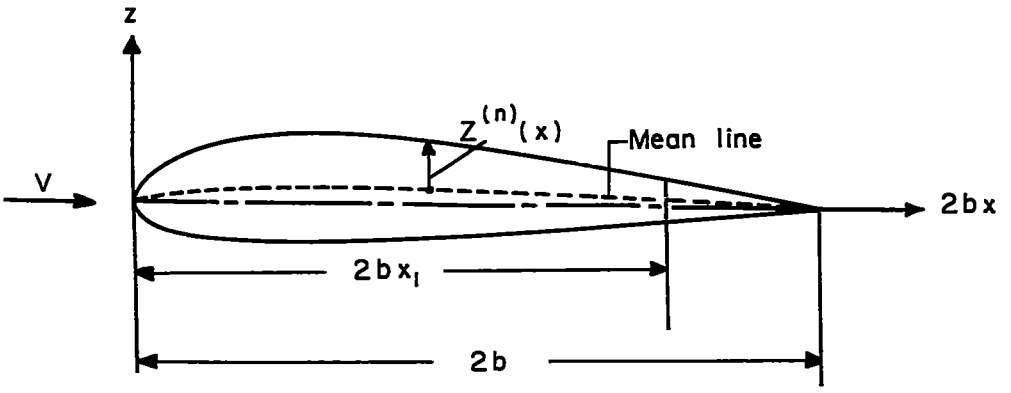

Figure 2.- Schematic drawing of geometric properties at any spanwise station of wing.

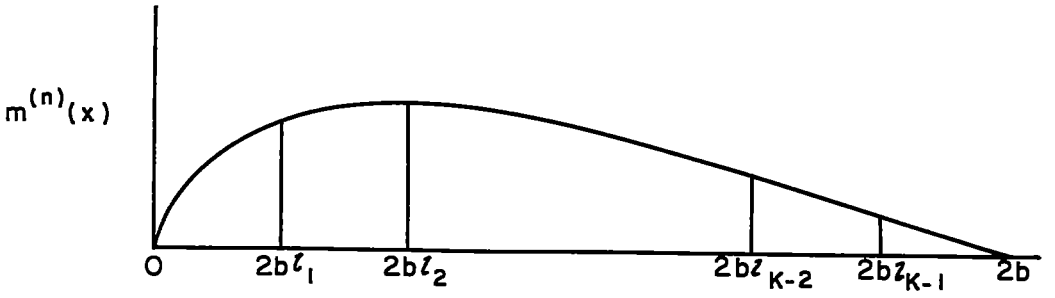

Figure 3.- Intervals for approximating chordwise mass distribution.

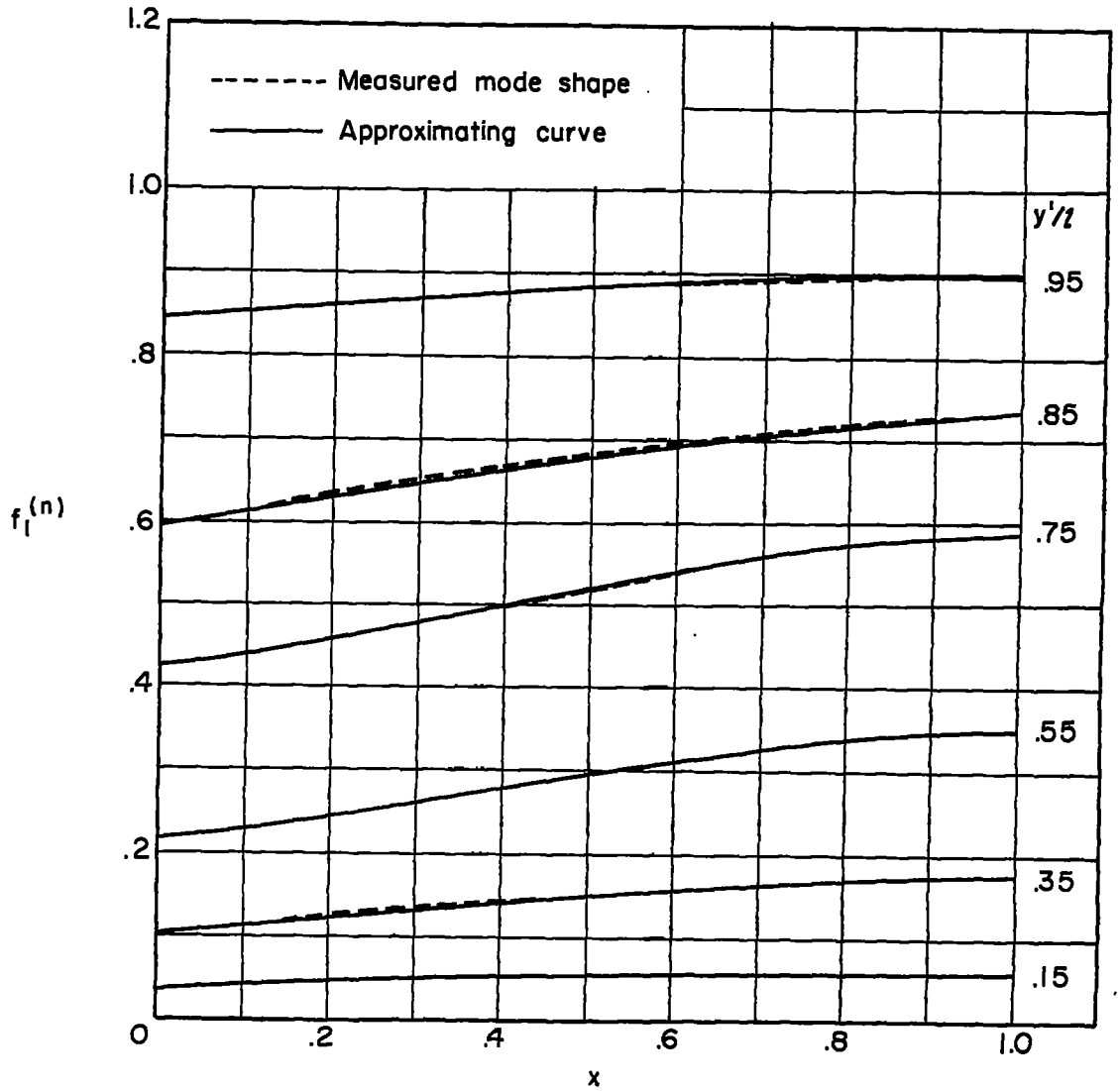

(a) First natural mode.

Figure 4.- Comparison between measured chord deflection mode shapes and their polynomial approximations for the first three natural modes of a 45° delta wing at various span stations.

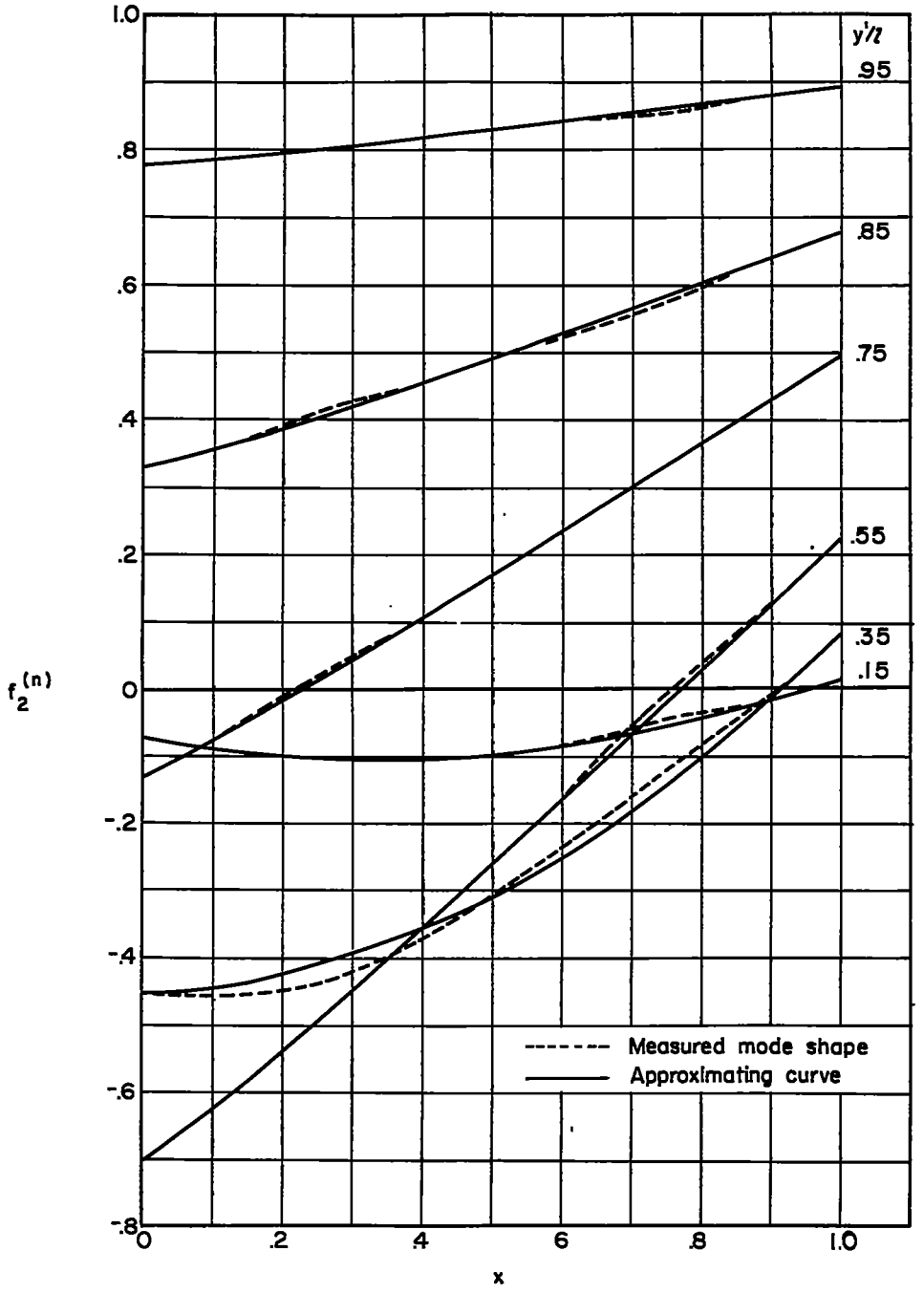

(b) Second natural mode.

Figure 4.- Continued.

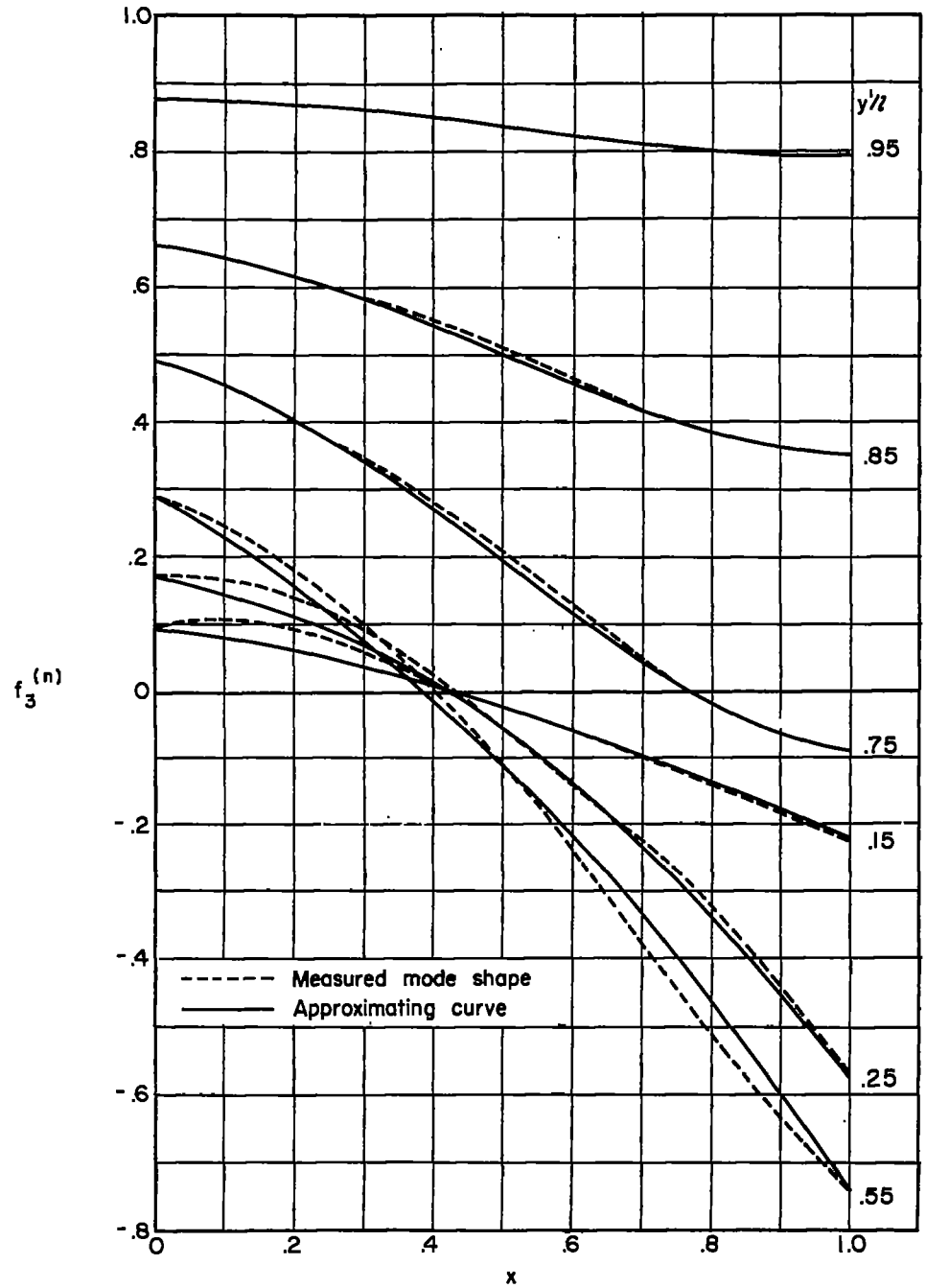

(c) Third natural mode.

Figure 4.- Concluded.

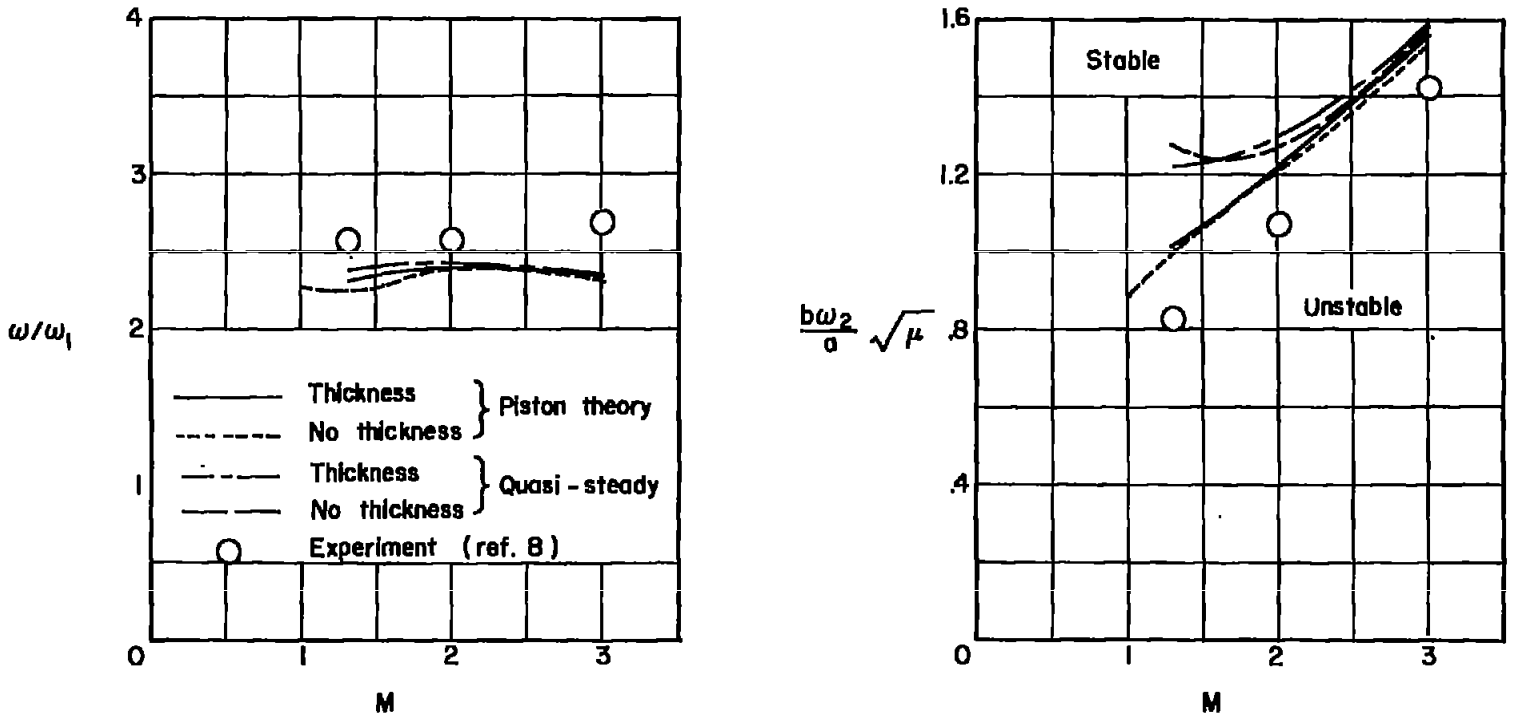

Figure 5.- Calculated flutter frequency ratio and stiffness-altitude parameter compared with experiment for a flat-plate 60° delta wing.

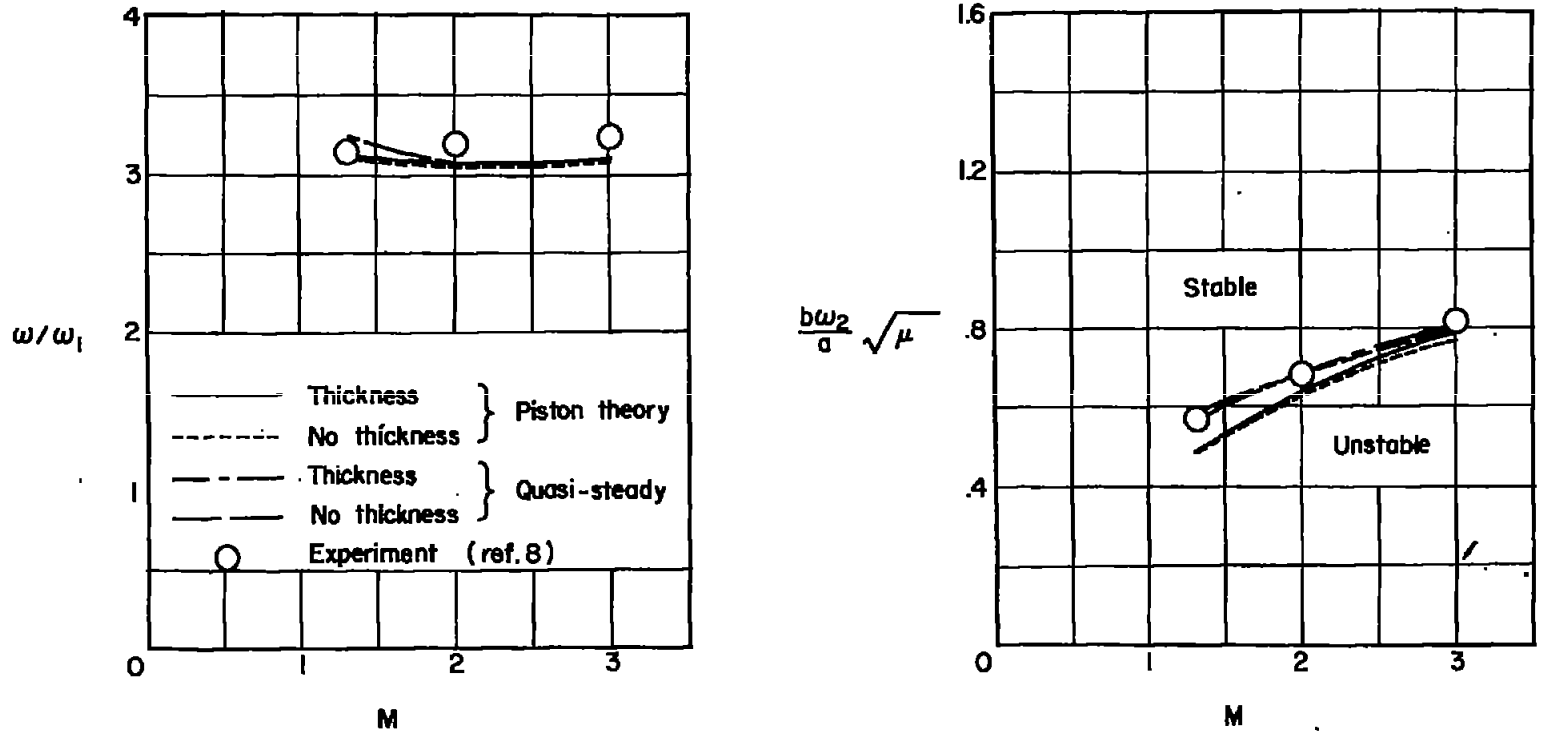

Figure 6.- Calculated flutter frequency ratio and stiffness-altitude parameter compared with experiment for a flat-plate 45° delta wing.

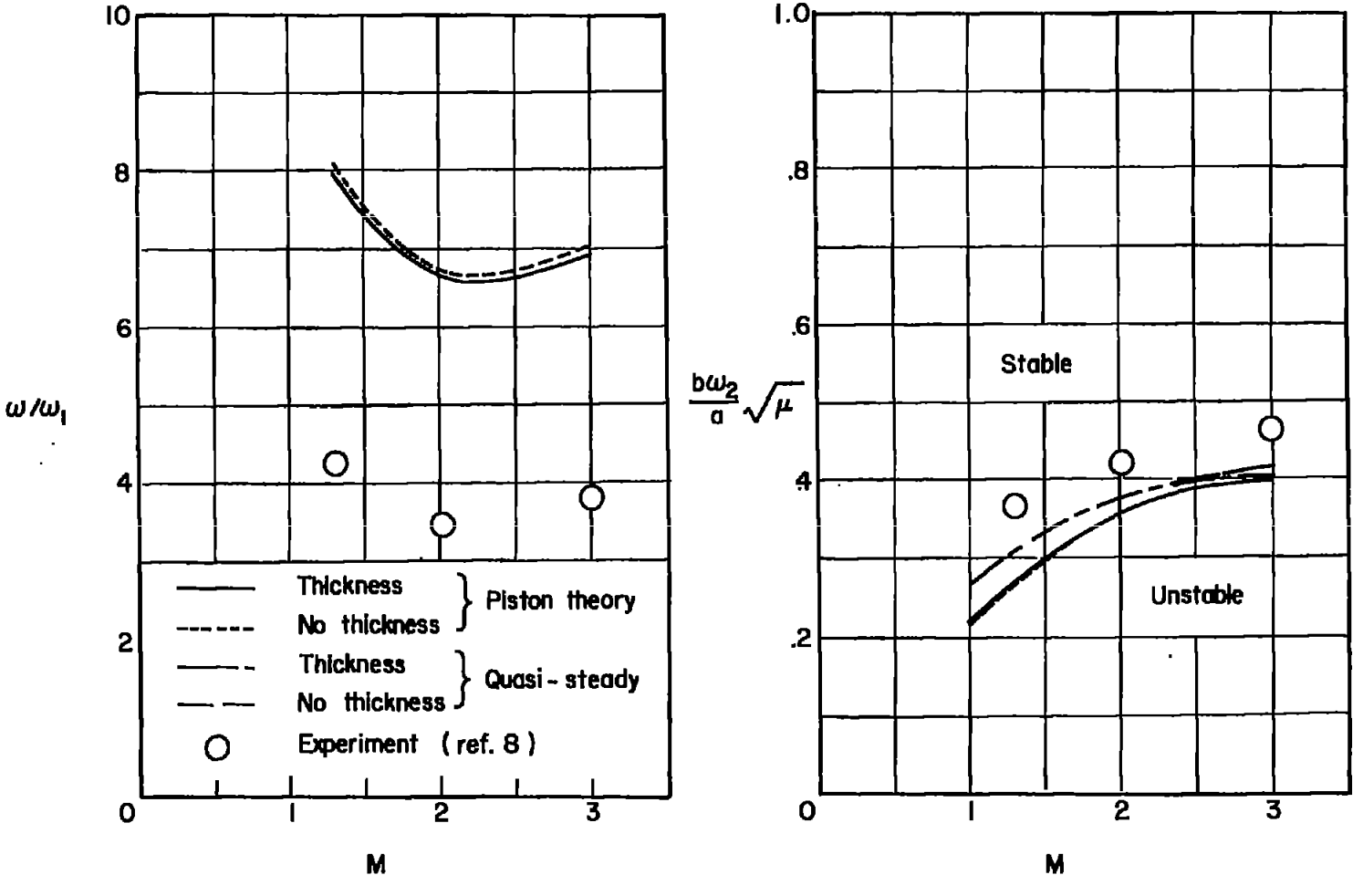

Figure 7.- Calculated flutter frequency ratio and stiffness-altitude parameter compared with experiment for a flat-plate 45° swept wing.

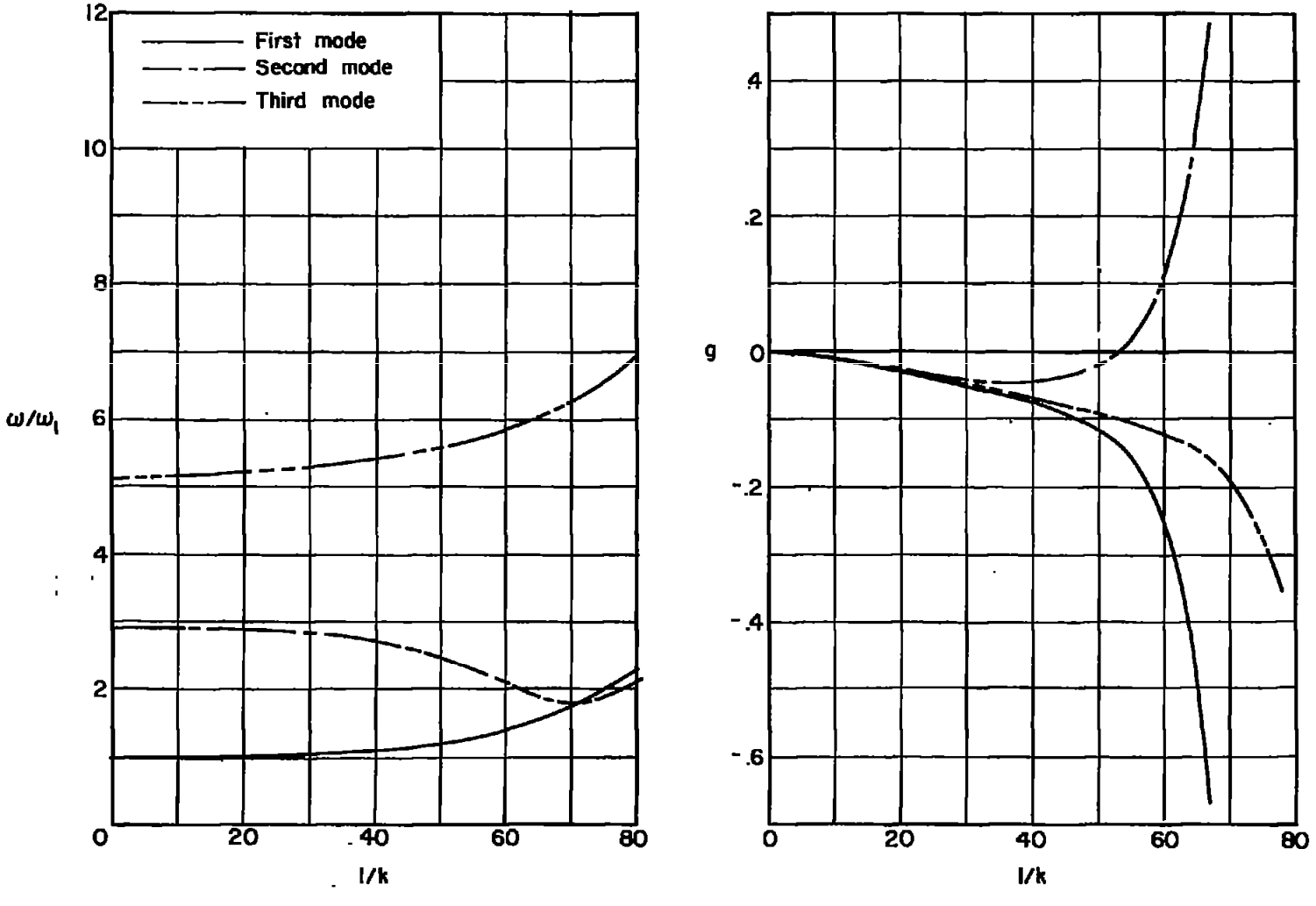

Figure 8.- Calculated frequency and damping in each mode for the example given in the appendix.